



Characterisation, activation, and reactivity of heterogenous natural clays

Amrita Hazarika · Liming Huang ·
Arezou Babaahmadi

Received: 29 November 2023 / Accepted: 7 March 2024
© The Author(s) 2024

Abstract Although thermal and mechanochemical activations of natural clays are well-documented, there exists a dual research gap. Firstly, a thorough investigation into the interrelationship between these activation methods and the governing parameters of reactivity for various clays has been notably lacking. Secondly, there is a distinct scarcity of studies specifically focusing on heterogeneous clays compared to the extensive research dedicated to single-layer clays specially kaolinitic clays. This study investigates the correlation of activation methods, and changes in the clay mineralogy, particle size distributions, morphology, specific surface area, and the reactivity of heterogeneous clays. Traditional thermal and mechanochemical activation methods often fall short in achieving complete dehydroxylation of heterogeneous clay minerals and improving their reactivity beyond predefined low thresholds. The results in this paper emphasize that, despite these limitations, combining these activation methods brings about significant modifications in crucial parameters. Notably, integrating 20 min of mechanochemical activation at 500 rpm with prior thermal treatment leads to 158% increase in specific surface area compared to mechanochemical activation conducted on un-calcined clays. Simultaneously, these combined activations

result in up to 127% improvement in reactivity levels of heterogenous clays compared to standalone mechanochemical activation. The results underscore that, even with the advancements brought about by combined activations, the presence of impurities like iron oxides and calcite remains a noteworthy factor influencing the reactivity of kaolinitic natural clays. The study concludes by highlighting the potential of combined treatments to enhance the pozzolanicity of low-reactive heterogeneous clays, unlocking avenues for future clinker supplementation with this abundant resource.

Keywords Heterogenous natural clays · Activation · Impurities · Reactivity

1 Introduction

Reducing the usage of clinker with alternative binder sources is one of the most practical ways to decarbonize the cement industry and bring it closer to net zero targets. Since the reserves of conventional supplementary cementitious materials (SCMs) such as blast furnace slags and fly ashes are limited and are increasingly getting depleted, the global focus has, over the current decade, pivoted towards natural pozzolans. As a vastly available and sustainable resource, previously untapped natural or common clays has been dominantly explored and highlighted over the past few years [1–10]. Raw and un-activated clays

A. Hazarika (✉) · L. Huang · A. Babaahmadi
Department of Architecture and Civil Engineering,
Chalmers University of Technology, Gothenburg, Sweden
e-mail: amrita.hazarika@chalmers.se



exhibit unsatisfactory pozzolanic behaviour and low technological performance, on account of the crystal stability of clay minerals. However, upon activation, the layered clay minerals (phyllosilicates) can undergo structural rearrangements, yielding partially disordered alumina and silica rich phases that contribute to their pozzolanic reactivity [11, 12]. Quite a number of activation techniques have been reported over the years, and the most common methods include the thermal activation and mechanical activation [12–18]. The optimal activation is achieved through amorphization of the clay mineral upon complete dehydroxylation of the octahedral sheet.

To achieve complete amorphization of the phyllosilicates, the favoured activation methods are commonly thermal activation (TA) or mechanochemical activation (MCA), because of the ease of operation, efficiency, and scaling up to industrial applications [13, 16, 18]. The TA process is characterized by dehydroxylations and decarbonation of the clay phyllosilicates under a high temperature regime in the range of 550–950 °C [13]. This process is observed to improve the dissolution kinetics of Al and Si elements in a saturated calcium hydroxide environment, resulting in an enhanced pozzolanic reactivity of calcined clay [19]. Industrially, furnace calcination is a much-favoured activation method because of the yield of output and ready availability of apparatus and technology.

Alternatively, some studies underline the advantages of MCA as an even more efficient and environmentally friendly activation strategy for clays [20–24]. This type of activation involves a source of mechanical energy such as a high-energy ball mill, to trigger physicochemical transformations including alteration of morphologies, particle sizes, surface charges, and creation of crystal defects, that leads to the reduced crystallinity of minerals. This accompanies higher specific surface area that lead to more reactive sites. Studies show that certain clay phyllosilicates such as illites, smectites, mixed layered illite-smectites, and sepiolite, which otherwise require relatively high temperatures beyond 900°C to dehydroxylate via calcination, are better amorphized under the intensive impact and friction-based grinding regimes of MCA [19]. Different parameters for MCA have been examined in previous literature. In general the pozzolanic potentials of mechanochemically activated heterogenous clays, especially with

2:1 minerals, ground at 500 rpm for up to 20 min at a ball to powder (B/P) ratio between 10 to 25, have been reported to be superior to the same clays that are thermally activated [22, 23].

Despite the advantages over one another in some respects, both activation methods have their own limitations:

- i High temperature calcination cannot effectively amorphize all 2:1 mineral phases, not at least below 900 °C. Possibilities under the increased temperatures have been checked earlier [7, 25]. However, since raw clays are multimaterials, calcining them at temperatures beyond 800 °C can recrystallize certain activated mineral phases and lead to a decrease in reactivity overall [26].
- ii The MCA technology is yet to be studied comprehensively for potentially low kaolinitic clays. It is much more studied in terms of synthesized or pure phase clays, and single layered natural clays [18, 21, 24, 26–29]. These findings cannot directly be translated for multimaterial and mixed-layered clays. This is because of vast difference in mineral compositions. Presence of varying impurity levels can also substantially influence the grindability of such clays, the resultant specific surface area and in turn, to affect the reactivity [30]
- iii For MCA, although longer and more intensive grinding regimes are known to yield extensive amorphization of clays, it can also lead to substantially higher agglomeration of particles [22]. This can then affect the reactivity. The common finding in terms of optimal grinding duration is about 20 mins, in at least 250 rpm for kaolinitic clays and 500 rpm for 2:1 clays to achieve the best activity, beyond which the clay starts to agglomerate [22, 23, 31], potentially resulting in a lower reactivity. However, this is also influenced by grinding parameters such as speed, ball to powder ratio, etc, that are necessary for activation [32].

Worldwide, the share of lower reactive 2:1 type minerals, mixed layered and low-kaolinite clays is comparatively higher than single layer clays [33]. This is especially the case in temperate, arid, and colder climates [34]. However, from the perspective of utilizing this



vast resource as a future binder, the investigation of their activation requires more attention. This is the first step to comprehensively harness their potentials for use as SCMs. Several comparative studies between thermal and mechanochemical activation have been conducted on kaolinitic and synthetic clays [22, 25, 33, 35, 36]. However, when it comes to natural mixed layered clays, such an archetypical approach may not work, especially if the idea is on maximising amorphization and reactivity.

In this context, thermal activation, mechanochemical activation, and combinations of thermal and mechanochemical activation (TA-MCA) treatments were systematically applied to explore how these activation methods alter the properties of heterogeneous clays and the subsequent impact on their reactivity. The combinations of TA and MCA were specifically designed to investigate whether they could further enhance the modification of these parameters, aiming to achieve higher reactivity for these inherently low-reactive pozzolans. The investigation focuses on understanding how activation methods influence crucial parameters, including clay mineralogy, particle size distribution, morphology, specific surface area, and their relation to reactivity. The sensitivity of these parameters to modification during activation directly impacts the extent of reactivity achieved by the clays. The clays under examination exhibit heterogeneity in mineralogy, encompassing 1:1, 2:1, and interstratified clay phases, along with impurities that can influence reactivity. The mineralogy of the clays was studied via X-Ray Diffraction (XRD), Thermogravimetric Analysis (TGA), Scanning Electron Microscopy (SEM) and Fourier Transform Infrared (FTIR) spectroscopy. Particle size was studied via laser diffraction, specific surface areas through Brunauer-Emmett-Teller (BET) analyses of nitrogen sorption, and reactivity via Modified R3 (MR3) method [35]. This study represents a concerted effort to unravel the activation requirements of heterogeneous clays, considering their composition and its potential effects on changes in particle size, surface area, and pozzolanic reactivity.

2 Materials and methods

2.1 Materials

The natural clays studied in this work were sourced from two locations in Sweden, one in the eastern

marine region of Norrköping in Östergötland, and the other in the southern region of Ängelholm in Skåne. They are hereby, respectively labelled as NC and SC. By sedimentation test, it was found that the clay content of NC is 80% and that for SC is 64%. The decision to select clays from these two regions is motivated from an earlier study that comprehensively analysed clays from 15 selected regions in Sweden [36]. It was found that the sedimentary clay in the south and marine clay deposits in the east offer the maximum pozzolanic potential for use as SCM. Furthermore, a lack of processing units that could deliver ready-to-use clays for this study, necessitated manual sourcing from specific locations. This resulted in the identification of limited locations that were accessible for excavation or capable of providing materials with the preferred mineralogy. Norrköping and Ängelholm represented the most readily accessible options for sourcing the heterogeneous clays, although more reactive alternatives, especially from the south of Sweden, are known to exist [36].

2.2 Test methods

The mineralogy of clays was characterized by XRD, TGA, and FTIR. To identify minerals in un-activated clays, XRD was collected on Rikagu Miniflex 600 in the 2theta range 1° – 30° with a scanning speed of 1° /min. For identification of clay minerals, dried sedimented suspensions of clay were used. To obtain this, particles below $2\ \mu\text{m}$ (clay fraction) was separated from the bulk material via sedimentation [36]. A suspension was first created by mixing 0.1 g of clay with 10 ml of deionised water, which was then dispersed via ultrasonication for 30 s. After 30 mins of allowing settlement of particles according to Stokes law, approximately 1 ml of suspension from a 3 mm depth to the top, was pipetted and placed on a clean glass film. The glass film is then dried in a desiccator, containing silica gel, at room temperature. After drying, this film is used for XRD test. In addition to this, the clay fractions were also treated with ethylene glycol to distinguish the swellable and interstratified minerals [37].

To study the effect of activations on the treated clays, XRD was conducted on activated as well as unactivated (powdered) clays. This was conducted on Bruker D8 Discover in the 2theta range 5° – 60° with step size: 0.02° , time per step: 0.8 s. 5% Corundum



was used as an internal standard. To quantify the clays, XRD Rietveld refinement was conducted on the unactivated clays. The analysis began by utilizing dried suspension samples to accurately identify minerals within the clays, employing the DIFFRAC.EVA V5.2 software for meticulous mineral identification within the clay matrix. CIF files corresponding to identified minerals were retrieved from the COD database and subsequently imported into TOPAS 32-V6. In the preliminary refinement phase, the background refinement was conducted in TOPAS 32-V6 utilizing Chebychev polynomials up to the 20th order. Simultaneously, for each mineral phase, background optimization was performed concurrently with the hkl files. The background parameters were then fixed for further Rietveld quantitative analysis. Adjustments to the crystallography of individual mineral phases within the CIF files were made based on hkl information prior to quantitative analysis. Notably, preferred orientation parameters were incorporated for each mineral phase, set at an order of 8, except for smectite, where an order of 2 was applied, to adjust the peak intensity. The refinement process utilized the pseudo-Voigt peak type. The similarity observed in the total clay content, as determined by QXRD, in comparison to results obtained through sedimentation analysis, provides additional assurance regarding the accuracy of the data. In case of NC, the Rwp and Rp are 2,74 and 2,04, while for SC these were 3,67 and 2,67 respectively. The quantified results are provided in Table 1.

The accuracy of quantitative X-ray diffraction (QXRD) for mix-layer clays has been noted as challenging in the literature [38]. The quantified amount of the internal standard served as a crucial metric for ensuring result accuracy. A comparison with initially used values not only validated the precision of the analysis but also facilitated the consideration of standard deviations associated with each quantified

amount. However, it is important to clarify that this work, while undertaken with meticulous care in mix-layer clay quantification, is not intended as an exhaustive guide for addressing intricacies in the quantification methodology. The focus of this paper aligns with specific objectives, providing valuable insights within its defined scope. For more elaborate efforts aimed at enhancing the accuracy of quantifications, further detailed work may be necessary in other research contexts.

The surface morphology of the activated clay particles was observed by scanning electron microscopy (SEM) using a FEI Quanta 200 FEG electron microscope. TGA curves of raw and activated clays was measured by TGA/DSC 3+, Mettler Toledo. Each measurement was performed on clays in an alumina crucible in a nitrogen environment. The clays were heated from 20 to 1000 °C with a heating rate of 10 °C /min. The ATR-FTIR spectra of the raw clays were collected on a PerkinElmer Frontier FT-IR spectrometer, in the middle IR (MIR) region, using 2 mg of material. The oxide concentration measurements were conducted on acid digested samples via Inductively coupled plasma atomic emission spectroscopy (ICP-AES). LOI was measured by TGA. ICP-MS and shown in Table 2.

The reactivity of both clays in this work was assessed with Modified R3 test with an isothermal calorimeter, as detailed in [39], that is categorically tailor made for assessing the reactivities of low grade pozzolans.

Laser diffraction was conducted using MasterSizer 3000 (Malvern Panalytical) at a rotation rate of 2010 rpm. The dry powders were dispersed in water. The material was added in a beaker until the obscuration was around 10% after which the first measurement was conducted. Thereafter, the beaker was ultrasonicated for 60 s to break lumps, after which two consecutive measurements are taken.

Table 1 Mineral quantification of the two clays

Minerals wt% ± 2	Kaolinite (COD: 1011045)	Smectite (COD: 9010163)	Illite (COD: 9013732)	Quartz (COD: 9000966)	Calcite (COD: 9005019)	Total clay %
NC	21	28	33	13	–	82
SC	17	18	23	19	16	58



Table 2 Chemical composition (by weight percentage) of the two clays

Oxides														
wt%	SiO ₂	Al ₂ O ₃	Fe ₂ O ₃	CaO	MgO	Na ₂ O	K ₂ O	TiO ₂	MnO	P ₂ O ₅	SrO	BaO	LOI	Total
NC	51.80	18.35	9.55	1.32	3.34	1.70	4.42	0.87	0.11	0.15	0.01	0.08	8.15	99.86
SC	50.50	15.55	6.70	6.62	2.63	1.36	3.85	0.77	0.09	0.17	0.01	0.06	11.2	99.53

2.3 Treatment and activation methods

The following present the preparation and activation methods used in the study. Table 3 at the end of this section provides a summary of all the activation methods.

2.3.1 Drying and grinding

The raw clays obtained from the sources were clumpy and saturated with moisture. They were dried at 80 °C until constant mass was achieved and then ground for 5 mins in a planetary ball mill (Retsch PM 100), at 200 rpm prior to activation.

2.3.2 Thermal activation (TA) or calcination

Calcining temperature was determined based on the thermogravimetry analysis of the raw clays, carried out at a temperature range of 0–1000 °C, under a dynamic N₂ atmosphere. The TG-DTG analysis presented in Fig. 3 indicates the mass loss pattern of the two untreated clays, reflecting the dehydroxylations in both clays. For both clays, most dehydroxylation related mass loss were observed before 750–800 °C. With this information the thermal activation regime was chosen to be 800 °C with a duration of 60 mins, as also reported in previous studies on similar clays [36, 40]. The duration of 60 mins is adopted as it is known to be the most optimal time for transforming crystalline clay minerals to amorphous states. Higher durations could result in recrystallisation of metakaolin [40]. Thermal activation of the clays weighing 100 g was carried out in a laboratory furnace (Nabertherm), from room temperature to 800 °C with an activating time of 60 mins.

2.3.3 Mechanochemical activation (MCA) without prior calcination

Mechanochemical activation was carried out in a planetary ball mill (Retsch 100PM), under the

recommended milling conditions previously reported in [41] for natural Swedish clays. A 500 ml grinding jar was filled with steel balls of 12 mm diameter, and uncalcined clay, at a ball-powder (B/P) mass ratio of 25 and was then subjected to milling for 20 mins, at 500 rpm. The selection of the MCA regime was influenced by the observed results in both [22, 41]. These findings highlighted increased clay particle agglomeration and reduced specific surface areas when grinding exceeded 20 min at 500 rpm, with a B/P ratio ranging from 10 to 25.

2.3.4 Combined activations (TA-MCA)

A set of thermally activated clays were further subjected to mechano-chemical activation with two objectives - firstly, to amorphize 2:1 phases that are still present in thermally activated clays, and secondly, refinement of particle size distribution and specific surface areas, to improve reactivity. MCA was applied for two varying durations to these clays: for 10 and 20 min, with the rest of the grinding parameters kept constant as presented in 2.3.3. The clays undergoing these combined activations of TA and MCA are labelled TA-MCA10 and TA-MCA20. Table 3 summarises the activation treatments presented in Sects. 2.3.2–2.3.4

3 Results

3.1 Mineralogy of raw clays

The mineralogical representation of clays through XRD analysis is presented in Fig. 1. It shows that the clays have multi-mineral phases. In the air-dried clays, peaks attributable to smectites, illite, kaolinite and some non-clay phases like quartz could be identified in NC, whereas SC mainly shows illite and kaolinite along with either illite/montmorillonite or quartz. Similar peaks were also identified in



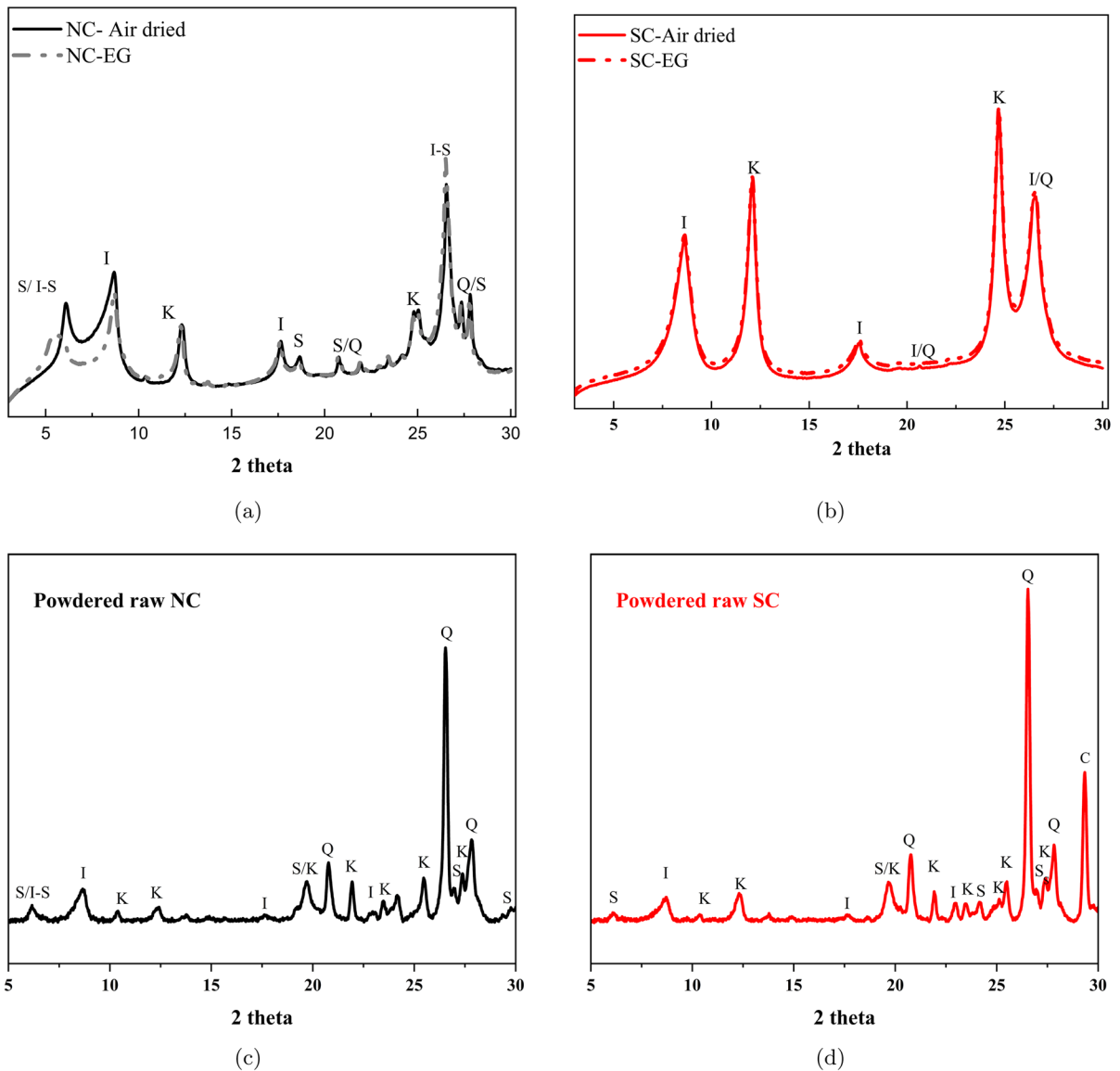


Fig. 1 XRD of raw suspensions: air dried and ethylene glycolated NC (a) and SC (b); XRD of untreated powders: NC (c) and SC (d); where, S = smectites, I = illite, K = Kaolinite, Q = quartz, I-S = interstratified illite-smectite, C = Calcite

Table 3 Activation methods adopted in study

Activation methods	Details
TA	60 mins of thermal activation at 800 °C in lab furnace on raw clays
MCA	20 mins of mechanochemical activation in ball mill, at 500rpm and B/P 25, on raw clays
TA-MCA10	10 mins of mechanochemical activation (500rpm, B/P 25) on thermally activated clay calcined at 800 °C
TA-MCA20	20 mins of mechanochemical activation (500rpm, B/P 25) on thermally activated clay calcined at 800 °C

the published works of [13, 19, 37, 42]. The curve of ethylene glycol treated SC does not show significant deviations from the air-dried clays. The diffractograms of NC show a clear shift of the peak from around 6° 2theta in the air-dried state to 5° 2theta in the ethylene glycol treated state, which is typical of either smectite, or interstratified illite-smectite [32, 42]. The intercalation of ethylene glycol in the expandable layers of these swellable minerals causes a shift in their XRD patterns after glycol treatment [42]. Peak at $26\text{--}27^\circ$ 2theta correspond to either illite or interstratified illite-smectite. For interstratified minerals, the ethylene glycol treated peak is shifted while for illites, this does not change [42]. Ethylene glycol treated NC shows a slight change of this peak which indicates the presence of interstratified illite-smectite. The diffractograms of the powdered un-activated clays (Fig. 1c, d) show the same clay mineralogy reflected in the synthesised samples. There is a calcite peak at around 28° 2theta shown in the powdered SC that does not appear in the synthesised samples. The reason could be because the synthesized samples wash away the calcite mineral.

Figure 2 presents FTIR bands of the two un-activated clays. The OH bands observed at 3700, 3650 and 3400 cm^{-1} are characteristic of kaolinite, while the band at 1635 cm^{-1} is attributable to illite or montmorillonite of the smectite group [32, 37]. The single band noticeable for only SC at 1430 cm^{-1} in the carbonate region is attributable to calcite [28]. There is a band in the Si-O stretching region at 1003 cm^{-1} typical of kaolinite, while the bands at 779, 689, 645, 530 and 429 cm^{-1} correspond to illite, kaolinite, and montmorillonite [34, 43]. From the mineral information provided by XRD and FTIR, the clays are clearly multiminerall by nature, or heterogenous.

From the TGA curves in Fig. 3, the mass losses at a temperature range of $300\text{--}800^\circ\text{C}$ relate to dehydroxylations of clay phyllosilicates [38]. It is known that the mass losses of these minerals commonly overlap in specific temperature intervals [37]. The mass loss observed for both NC and SC in range of $300\text{--}550^\circ\text{C}$ typically corresponds to 1:1 minerals like kaolinite, but also 2:1 phases of montmorillonite and illite. Therefore, the dehydroxylation peak here could be brought about by either kaolinite alone or collectively by 1:1 and 2:1 minerals present in the clays. Some other phases like calcite as shown in the FTIR for SC, could also start to decompose at this temperature range

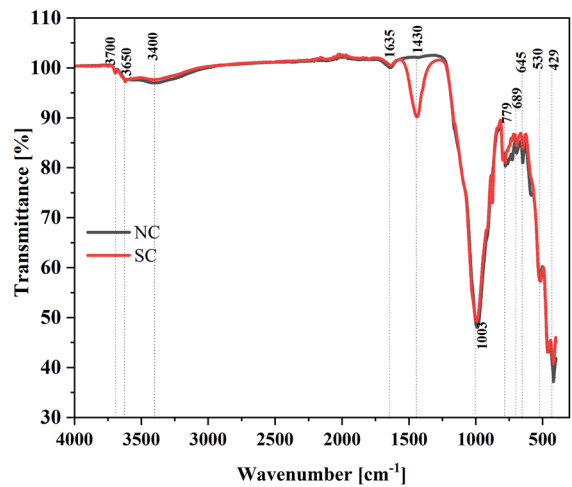


Fig. 2 FTIR spectra of the un-activated clays

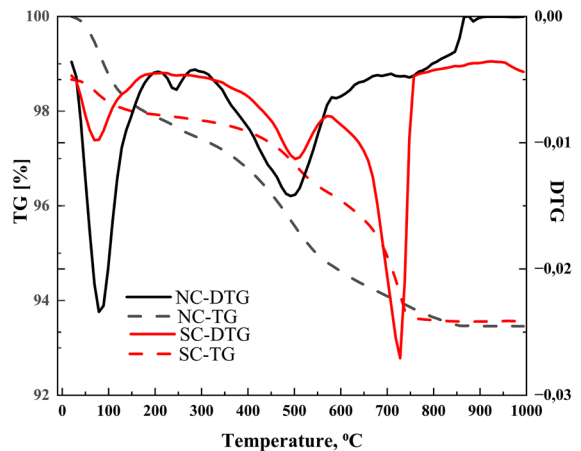


Fig. 3 TGA and DTG of the raw clays

[38]. SC has another dehydroxylating peak at 760°C that could be attributable to montmorillonite or illite. FTIR data for SC suggested the presence of both illite and montmorillonite while the XRD shows only illite. Hence, the dehydroxylating mineral in this range could be narrowed down to illite. Generally, the decomposition of SC occurs at a higher temperature compared with NC. This implies that SC is more stable than NC regarding the sensitivity to thermal activation treatment.

3.2 Mineralogy of activated clays

The XRD patterns of all activated clays, presented in Fig. 4, demonstrate reductions in peak numbers

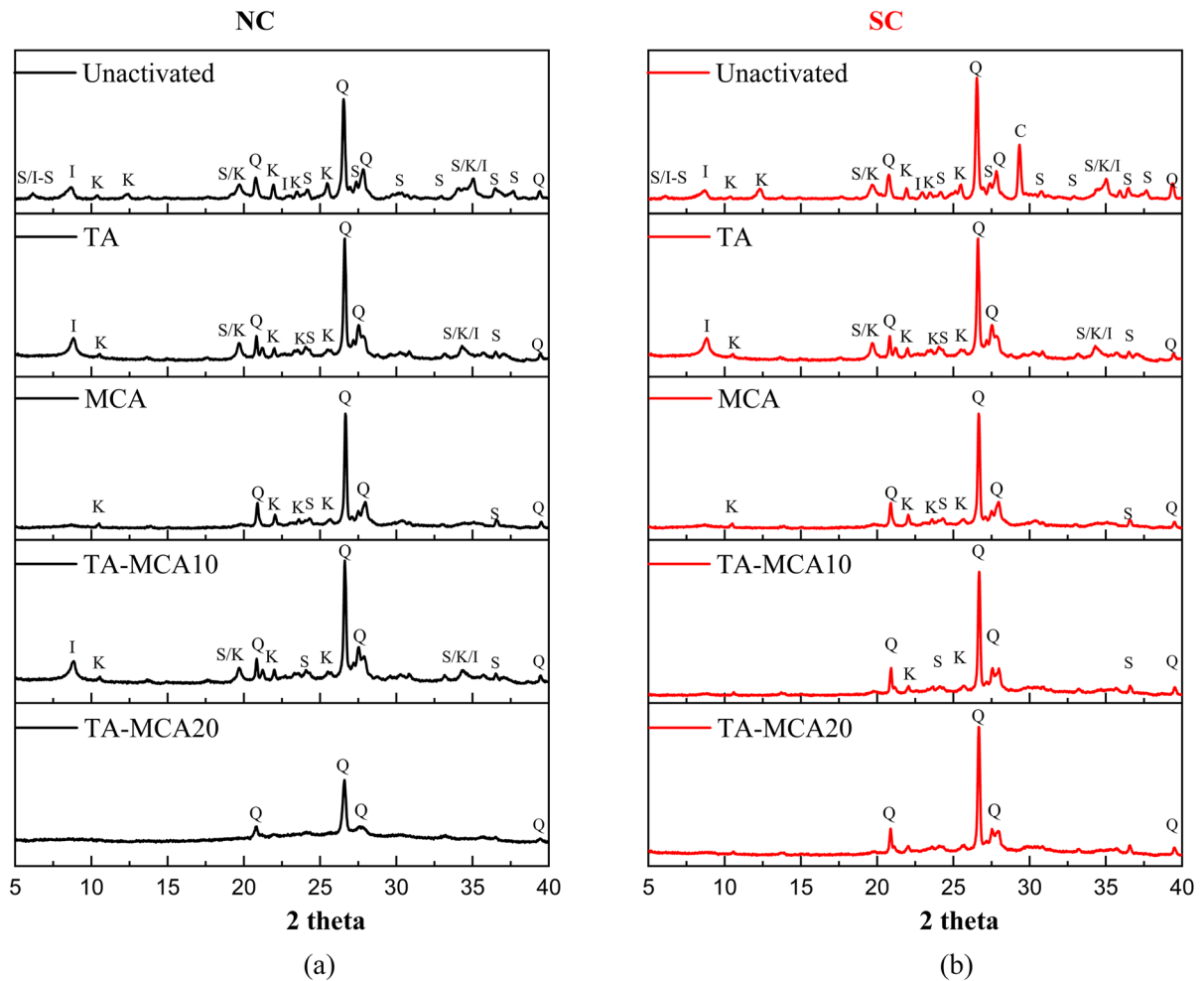


Fig. 4 XRD patterns of activated and un-activated NC (a) and SC (b). The mineral phases of interest are S=smectite, I=illite, K=kaolinite, I-S=illite-smectite, C= calcite, and Q= quartz

compared to their respective un-activated forms. For both the clay types, kaolinite peaks appear to get weaker after the thermal activation. In NC, the peak of smectite/illite-smectite, corresponding to around 6° 2θ , is absent after the thermal activation. The smectite peaks at around 20° and 35° 2θ , and the illite peak at 8° 2θ are still present after thermal activation. Similarly for SC, the illite and smectite corresponding peaks remain strong in the thermally activated sample. For both clays, diffraction of MCA samples appears to have no clear peaks corresponding to the clay minerals. This is also the case when MCA is conducted for 20 mins on previously thermally activated clays. However, with a reduced duration of MCA on thermally activated clays peaks of

illite and smectite could still be observed, as in the case of TA-MCA10 clays. Nevertheless, the decrease in peak strength implies the reduction in crystallization degree in these clays [14].

TG and DTG curves of the activated clays are presented in Fig. 5. Thermally treated clays show the least mass loss on account of increased dehydration and dehydroxylations under the high temperature calcination treatment. Compared to the MCA treated clays, the curves corresponding to the combined treatments show lower mass losses because firstly, the clays were initially thermally treated which dehydrated most free and bound water and secondly, due to further dehydration during the amorphization of clay minerals [22]. In the TA-MCA treated clays, the

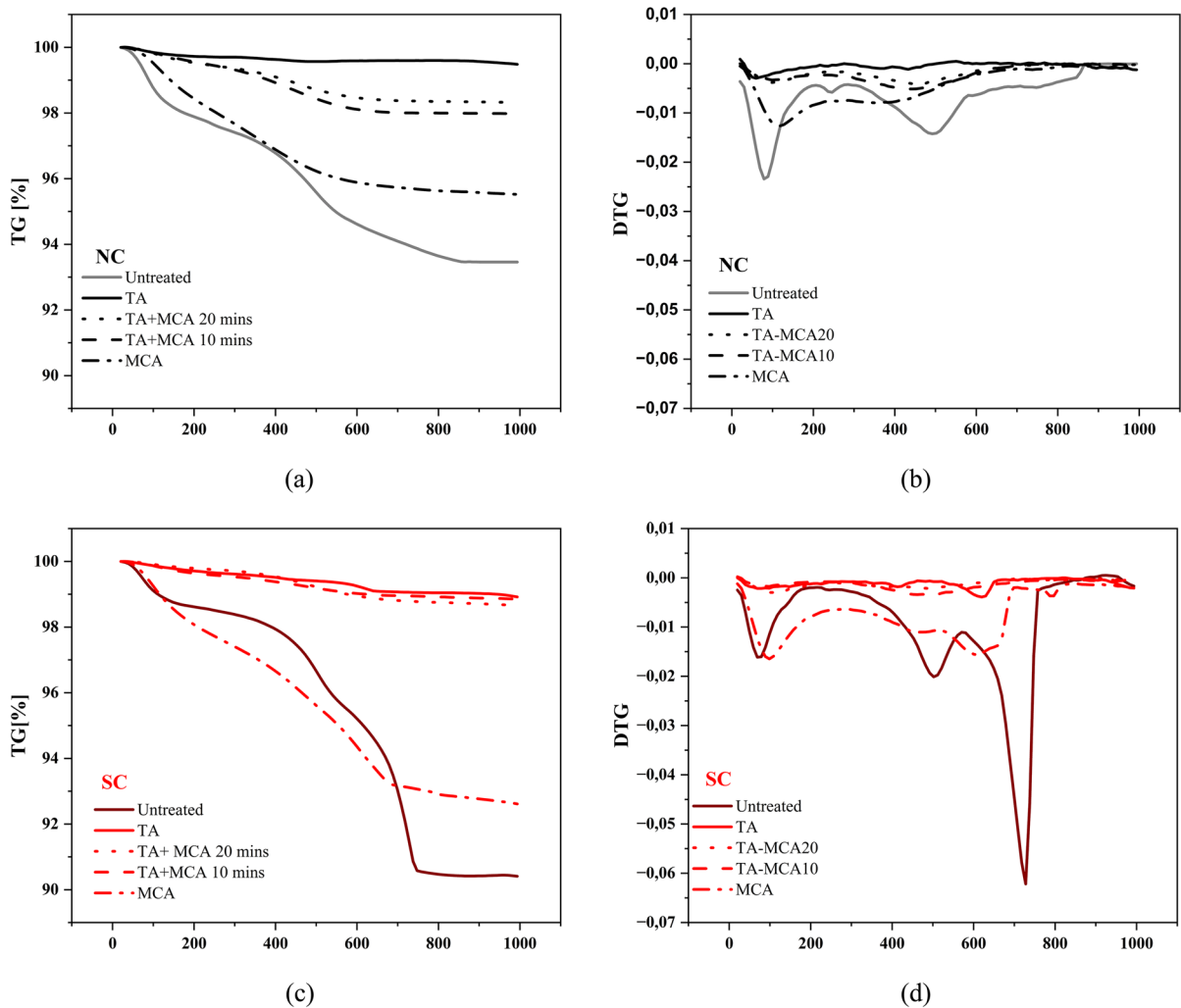


Fig. 5 TGA and DTG of NC (a) and (b), and of SC (c) and (d) respectively

significantly reduced or even absence of the mass loss peaks corresponding to clay minerals, matches the disappearance of crystalline peaks in the respective XRD of clays. In case of NC, some unexpected mass loss can be observed for combined treated samples around 550–600°C. This loss might be attributed to water absorption under exposure to atmospheric air, during the time interval between thermal activation and mechanochemical activation. In case of any new phases being created, this would have been detected in XRD. Future studies could investigate the influence of time intervals between the combined treatments.

3.3 Morphology of activated clays

Figure 6 demonstrates the morphological changes as the clays underwent the different activation treatments. Since these observations were similar for both clays, only one set of images comprising of representation from both clays, are presented in Fig. 6. for further discussion. The images for the other clay are presented in Appendix A Fig. 9. In general, it was observed that un-activated sample had bigger plate-like structures on which smaller lamellar structures were agglomerated. From previous research, it is known that thermal activation does not produce drastic changes in the intrinsic phyllosilicate morphology [22, 26]. In this study, it has been also observed that

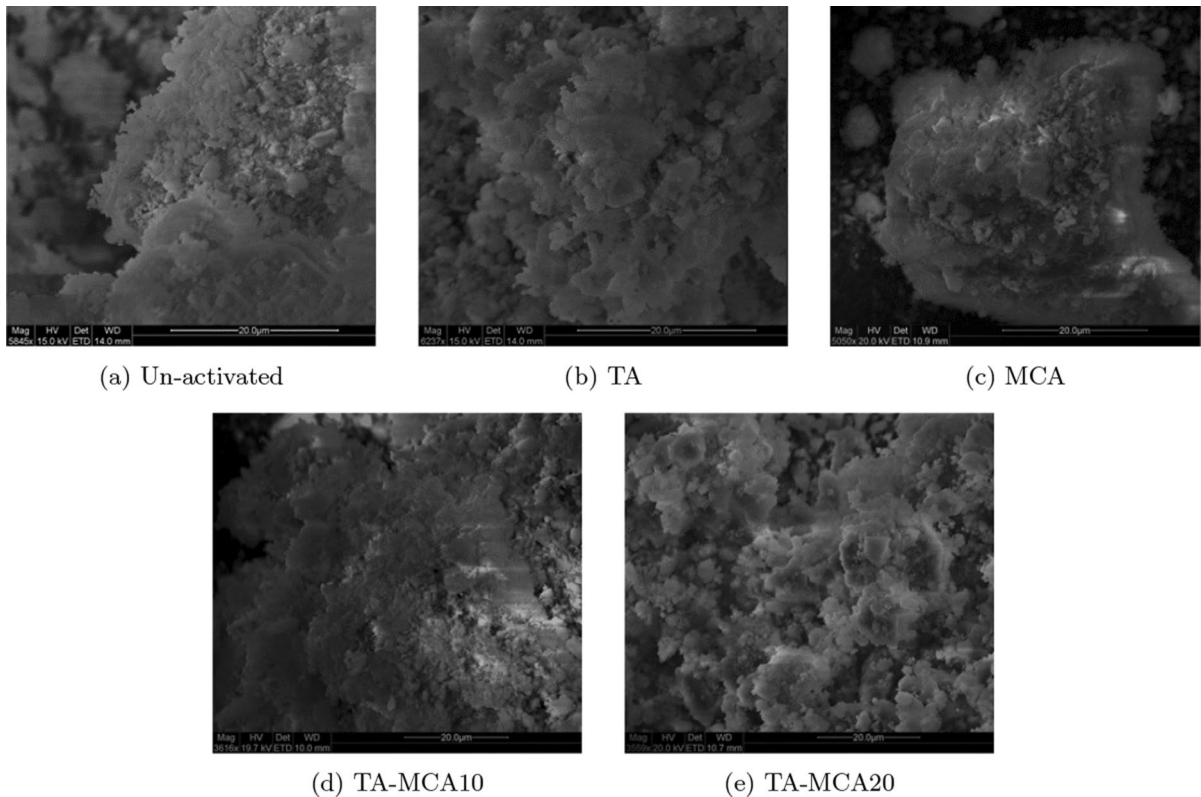


Fig. 6 Surface morphology of un-activated (a) and activated (b–e) NC clays

the agglomeration state is similar between the thermal activation and un-activated clays. Smaller clay particles appear to adhere on bigger particles for both TA and un-activated clays. MCA seemed to produce less agglomeration, and more round edged particles, distinguishable from one another. There is less agglomeration observed for thermal activated clays that underwent at least 10 mins of MCA. 20 mins of MCA on TA clay further produced more rounded and individual particles and distinctly less agglomeration.

3.4 Particle size distribution and specific surface area

The particle size distribution for clays is presented in Fig. 7, and particles in all samples exhibit bi or tri-modal distributions. This is owing to their inherent heterogeneity [9, 22, 26, 44, 45]. In general, the particle size distribution is relatively similar for the two clays, even across the different activation methods. The major modal distribution that observed at 100–350 µm is typically attributable to agglomeration of particles during the activations [46]. It can

be observed that for both clays, the introduction of MCA shifted this modal distribution to finer particle size ranges, and the volume of finer particles increased. MCA on previously thermally activated clays shifted the respective main peaks of the clays to finer size distributions. Compared to the raw and thermally treated clays, the most apparent change in the particle size distribution (PSD) is observed in the case of TA-MCA20 curves, where the tri-modal distribution becomes less pronounced and mostly resembles a bi-modal distribution. The particle size distribution analyses provided the D50 values of the unactivated and activated clays. The D50 of unactivated NC is 50,5 µm and of SC is 43,6 µm. Figure 8 presents the D50 values and the BET specific surface areas of the treated clays in relation to the different activation treatments. The D50 values progressively decrease as MCA is applied to previously calcined clays, in the increasing order of time durations. The BET specific surface areas appear to follow a similar trend, where for both the clays, the highest specific surface areas are observed for the ones with smallest

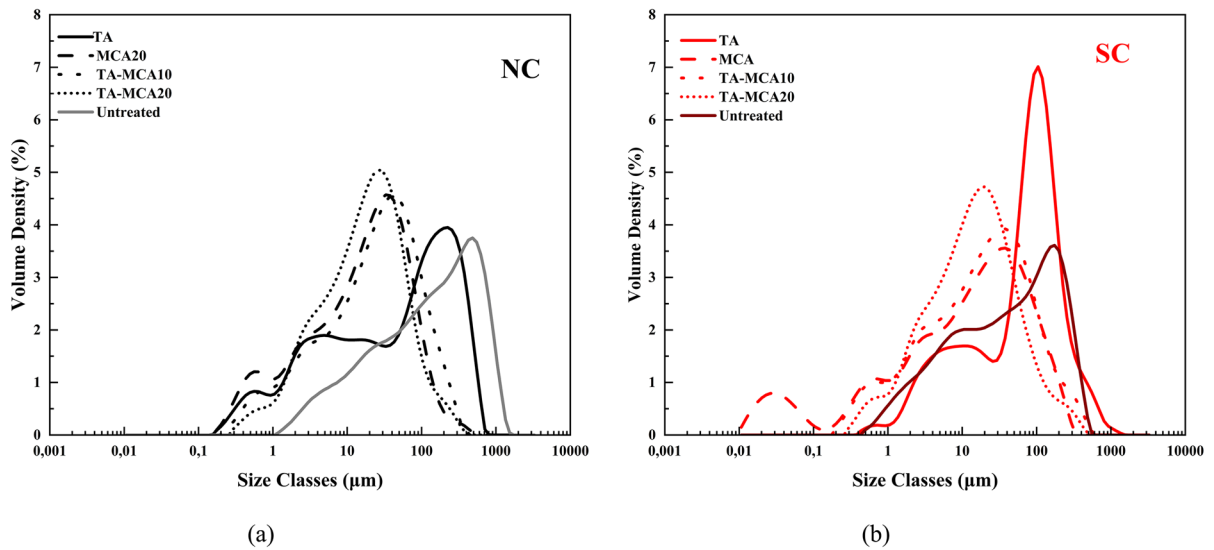


Fig. 7 Particle size distributions of clays before and after activations

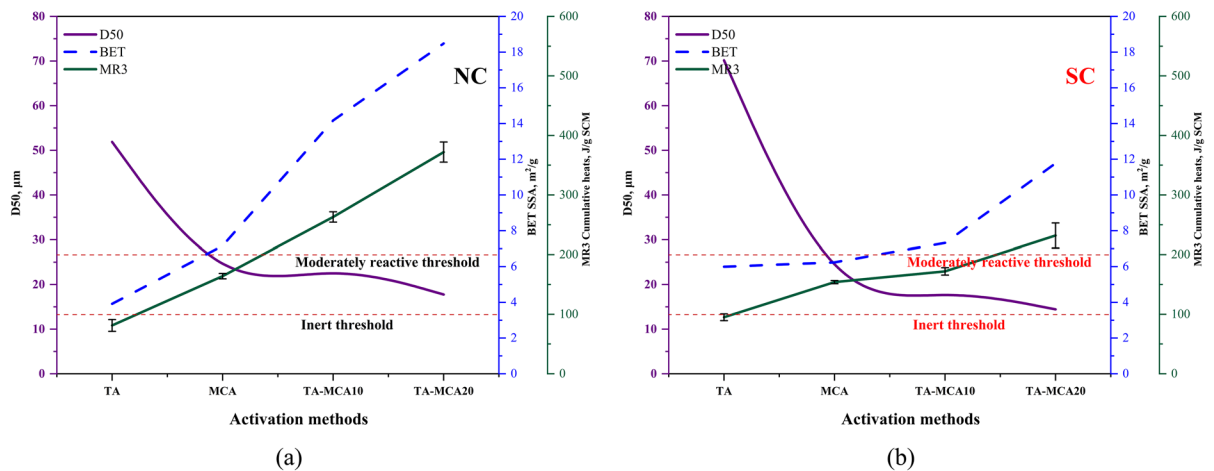


Fig. 8 Reactivity of NC and SC, in relation to BET specific surface areas and D50. Left hand axis shows D50 values obtained from particle size distributions. Blue right-hand axis

shows BET values. Green right-hand axis shows cumulative heat measured via Modified R3 test. (Color figure online)

D50 and corresponding to clays having the maximum energy input for activation (TA-MCA20). For NC, the TA-MCA10 increases the BET specific surface area of clay by 262% compared to TA clays and by 98% than MCA clays, whereas TA-MCA20 increases the surface areas by 374% compared to TA and 158% compared to MCA. For SC, the TA-MCA10 increases the surface areas by 22% in contrast to TA and 17% in comparison to MCA, whereas TA-MCA20 increase this by 95% than TA and by 87% in case of MCA.

3.5 Reactivity of activated clays

The cumulative isothermal heats of activated clays from the MR3 test are presented in relation to BET specific surface area and D50 of the treated clays Fig. 8. For activated clays, a higher cumulative heat normally represents higher pozzolanic activity and a potential for enhanced strength development [32, 44]. The threshold for screening inert versus reactive pozzolans is typically determined to be at 100 J/g SCM [45]. SCMs having total heat release lower than 100

J/g is classified as inert, or non-reactive materials. Two more reactivity thresholds generally accepted in the arena of calcined clay research are - firstly, a range of 200 J/g - 600 J/g SCM cumulative heat release corresponds to moderately reactive, and secondly, cumulative heat higher than or equal to 600 J/g SCM corresponds to the highly reactive pozzolans [45, 47]. The MR3 test results for both the clays are also presented in Appendix B, Fig. 10. The clays, especially NC, are not sufficiently reactive via thermal activation, at least as indicated by the R3 standards. The calorimetric curves of all clays are presented in the supplementary information. MCA is seen to contribute to a strong improvement of properties of clays which results in a significant higher reactivity for both the clays. This is supported by lower D50 and higher BET values, along with diminishing of crystal peaks observed in XRD pattern. MCA on previously calcined clays seems to improve these parameters even further, and especially in the case of NC. It is observed that NC reaches moderate level reactivity with 10 mins of MCA conducted on previously calcined clays. For SC, it takes a longer MCA on calcined clay to reach the moderate level reactivity. For NC, TA-MCA10 increased the reactivity by 60% compared to MCA and by 224% in contrast to TA. The TA-MCA20 treatment further raises these reactivities by 127% compared to MCA and 353% higher than TA. In the case for SC, TA-MCA10 increased the reactivity by 12% compared to MCA and by 81% with respect to TA. Thereafter, TA-MCA20 increases the reactivity by 50% compared to MCA and by 144% compared to TA.

4 Discussion

This research endeavours to unravel the intricate correlation between existing clay activation strategies, focusing on the effects on mineralogy, particle size distribution (PSD), and specific surface area and their correlation to reactivity (R3 method) of heterogenous natural clays. Notably, the study emphasizes that conventional thermal and mechanochemical activation methods alone prove insufficient in producing sufficient reactivity for these clays to serve as viable replacements in future cement applications. In contrast, the combination of thermal and mechanochemical processes has emerged as a promising approach, demonstrating enhanced reactivity in studied clay

types. In the light of this finding, the ensuing discussion centers around three compelling questions that arise from the study:

(i) *Why the combined activations produced comparatively higher levels of reactivity than TA or MCA?*

MCA on previously calcined clays have shown more positive outcomes in terms of reactivity. The introduction of intensive milling on already thermally activated clays significantly elevated specific surface area because of particle fragmentation. In case of TA treated clays the dehydroxylation of certain mineral phases appeared incomplete as seen from XRD patterns. This resulted in the reactivities below inert threshold. It was further seen that MCA alone was unable to produce the same effect as TA-MCA on performance of treated clays. This points to a possible contribution of the thermal activation process towards enhanced reactivity in the combination treatment. It is known that thermal activation is accompanied by sintering and agglomerations rising from the heating and cooling actions involved. It is reported that, the contraction from cooling can suppress agglomerating tendencies, wherein, the resulting PSD of a thermally activated clay can be finer than an un-activated clay [22]. Subjecting such a thermally activated clay to mechano-chemical grinding, can cause further fragmentation and fracturing, thereby increasing surface areas. Increased surface areas create new reaction sites that elevate the overall pozzolanicity. Therefore, thermally activating the clay and sufficiently cooling them prior to MCA, can promote reactivity of low-grade clays. The cooling rate is a parameter that can be further considered in future studies. Another point in relation to this is that both MCA and TA-MCA treatments result in nearly similar D50, but the combination treatments produce at least a minimum of 17% increase in specific surface areas in SC and a minimum of 98% increase in case of NC. Increase of surface areas is not necessarily resulted from finer particle sizes, as this can be possible from altered/fractured morphology instead, such as from creation of mesopores [48]. As a result, the PSD could still be similar while more specific surface areas become available for reaction in a morphologically altered sample. This altered morphology appears to be synchronous with higher reactivities produced under the combination activations.



(ii) *Why did the combined activations yield only in a moderate level reactivity in clays?*

The reason why even the most intense combination activation (TA-MCA20) failed to result in highly reactive clays, could be because of their inherent compositions. It was observed from the characterizations, that both clays consist of 2:1 minerals along with impurities such as calcite, iron oxides and quartz. Due to the heterogenous composition of the clays, they are intrinsically low reactive pozzolans than pure clays that can demonstrate higher reactivity levels. Additionally, it is known that iron oxide impurities present in clays, might deter the dissolution of aluminum (Al) during the amorphization process [49, 50]. The water molecules that are dehydrated during an activation process leaves behind vacant sites that are usually filled by Al ions. The transfer of Al to the vacant sites leads to the destabilization of the alumina-silica layers that ultimately transforms the mineral kaolinite, to its reactive phase - metakaolin. However, the existence of iron impurities, can hinder this process by forming a coating, thereby leading to an incomplete metakaolin conversion [51]. Inadequate conversion of the clay's most reactive mineral phase (kaolinite) can hinder the achievement of higher reactivities.

(iii) *Why is there a difference between the reactivity of the two clays, despite undergoing the same combined treatments?*

The two clays have achieved varying levels of reactivity, especially noticeable after the combination activations. It was seen that TA-MCA10 for NC yielded moderate level reactivity, but SC required longer (twice the duration) MCA for reaching this level. The reasons behind this differential reactivity can be traced to two aspects: compositions of the two clays, and the difference in specific surface area attained by the two clays under the treatments. In terms of reactivity of clay minerals, they follow the order illite < smectite < illite-smectite < kaolinite [32, 52]. Quantified XRD analyses reveal a higher proportion of the higher reactive minerals in NC compared to SC.

Furthermore, after the TA-MCA10 treatment, NC exhibited a 94% increase in specific surface area compared to SC, and a 57% increase with the TA-MCA20 treatment. This heightened specific surface area correlates with increased reactivity in NC. The lower specific surface area observed in SC may be attributed to the presence of calcite, as indicated by FTIR

spectra. The presence of calcite is known to induce calcium deposition on metakaolin particles, diminishing specific surface area and potentially impairing reactivity [30, 53].

While combination treatments can alter factors like particle size distributions and specific surface areas, the intrinsic heterogeneity of clay compositions (mineralogy and impurities) seems to impose limitations on the extent to which reactivity can be influenced through activations.

5 Conclusion

This study delves into understanding limitations of the two widely reported activation methods-thermal activation (TA) and mechano-chemical activation (MCA)-in the context of heterogeneous clays. A combination of TA and MCA methods was also studied in relation to its effect on two types of heterogenous clays. Our investigation aimed to establish a nuanced relationship between currently practiced clay activation methods and changes on key parameters such as clay mineralogy, particle size distribution, and specific surface area, in correlation with the reactivity of clays. The ensuing discussions present critical insights and draw significant following conclusions from these observations:

1. Conventional activation strategies of TA and MCA are not sufficient to reach even moderate reactivity levels for heterogenous natural clays. Both clays narrowly cross the inert threshold of 100 J/g SCM (as per R3 isothermal calorimeter test) after TA and are still in low reactive levels (100–200 J/g SCM) after MCA.
2. A combined TA-MCA treatment resulted in modifications of morphology, particle size distribution, and specific surface area. In these respects, TA-MCA20 was found to be the most effective treatment among those tested. In NC, this combined activation increased the specific surface area by up to 374% compared to TA and 158% compared to MCA. In SC, this number was 95% higher compared to TA and 87% higher than MCA.
3. In the TA-MCA process, incorporating TA before MCA proves beneficial for enhancing the reactivity of heterogeneous clays, surpassing the reactivity achieved through MCA alone. In the case of NC, the reactivity of the combined activated

clay exceeded that of the MCA clay by 127%, while for SC, the improvement was 50%.

- The difference in the reactivity levels achieved by the two clays is governed by their intrinsic mineralogical and impurity compositions. The lower proportions of clay minerals, particularly kaolinite, in conjunction with the presence of impurities such as iron oxides and calcite, contribute to the suppression of reactivity. These impurities not only hinder the amorphous capacity of metakaolin but also lead to a reduction in the specific surface areas

Acknowledgements The authors would like to acknowledge financial support received from FORMAS, the Swedish Research Council, for the study New era for cement replacement materials: Importance of service life design (NewDurCem) with grant number: FR-2020/0008, the Family Thomas Foundation for the project: Evolution of pozzolan incorporated concrete: resistance to carbonation (Carbo-crete), and Vinnova (Sweden's Innovation Agency) for the project: Towards a climate neutral and resource efficient soil stabilization additive, with grant number: 2021-01053, (the work is carried out within the strategic innovation program InfraSweden2030, a joint initiative by Vinnova, Formas and the Swedish Energy Agency). The authors sincerely thank the contributions and assistance of personnel and faculty at the following institutes:

Gilles Plusquellec, Emilie L'Hopital and Ojas Chaudhari at RISE Research Institute of Sweden; Birhan Alkadir Abdulahi for assistance with BET measurements, Amir Saeid Mohammadi along with the faculty of SEM and XRD at CMAL (Chalmers Materials Analysis Lab), Per Lindh as well as Lars Nilsson for providing the clay samples and Klaartje de Weerd as well as Luping Tang for the co-supervision. The authors sincerely thank the contributions and assistance of personnel and faculty at the following institutes: Gilles Plusquellec, Emilie L'Hopital and Ojas Chaudhari at RISE (Research Institutes of Sweden at Borås); Birhan Alkadir Abdulahi for assistance with BET, Amir Saeid Mohammadi along with the faculty of SEM and XRD at CMAL (Chalmers Materials Analysis Lab), Per Lindh and Lars Nilsson for providing the clay samples, and Klaartje de Weerd as well as Luping Tang for the co-supervision.

Funding Open access funding provided by Chalmers University of Technology.

Declarations

Competing interests None.

Appendix A: ESEM images for SC

Figure 9 presents the SEM images for SC activated under the different activation methods.

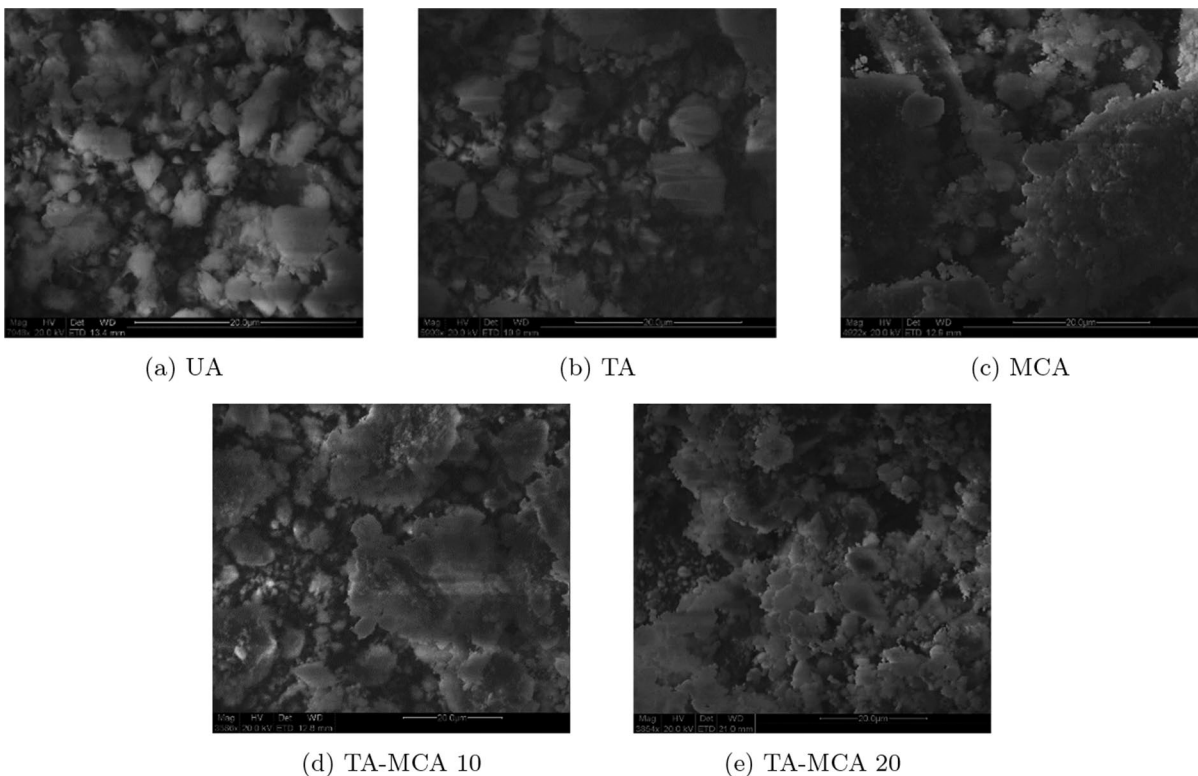


Fig. 9 Figure showing ESEM images for SC for different activation methods



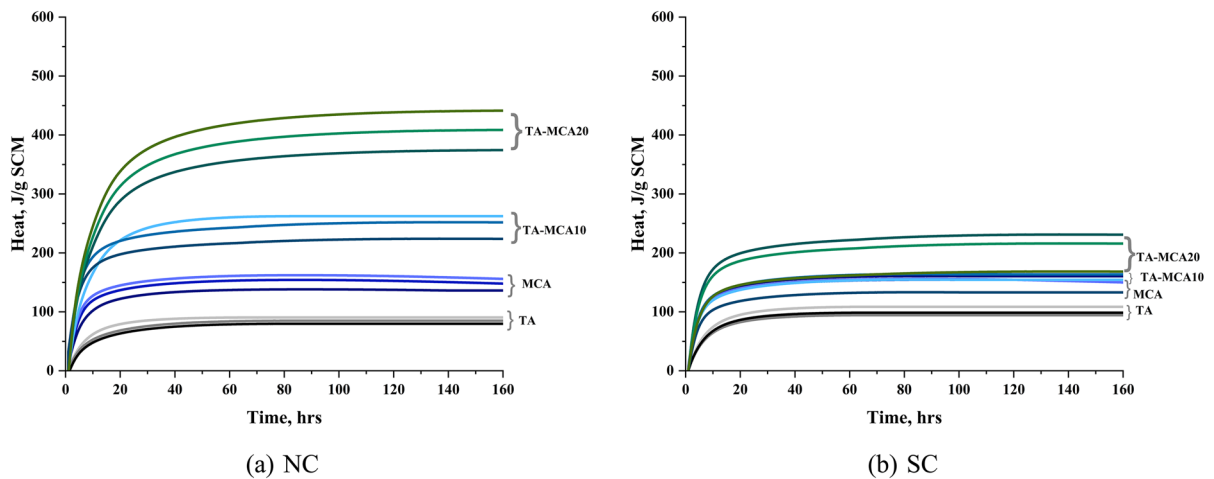


Fig. 10 Figures showing reactivity curves for NC and SC using different activation methods

Appendix B: MR3 reactivity curves for NC and SC

The MR3 tests for both clays (NC and SC) under the four activation treatments described and examined in the study, are presented in this section. For each activation, two repetitions were conducted to a total of three test results. The plots in Fig. 10 show the three results for each activation method performed for each clay.

Open Access This article is licensed under a Creative Commons Attribution 4.0 International License, which permits use, sharing, adaptation, distribution and reproduction in any medium or format, as long as you give appropriate credit to the original author(s) and the source, provide a link to the Creative Commons licence, and indicate if changes were made. The images or other third party material in this article are included in the article's Creative Commons licence, unless indicated otherwise in a credit line to the material. If material is not included in the article's Creative Commons licence and your intended use is not permitted by statutory regulation or exceeds the permitted use, you will need to obtain permission directly from the copyright holder. To view a copy of this licence, visit <http://creativecommons.org/licenses/by/4.0/>.

References

- Anders L, Antoni M, Diaz A, Hernandez J, Scrivener K (2015) Effect of fineness in clinker-calcined clays-limestone cements. *Adv Cem Res* 27(9):546–556
- Adrián Alujas, Roger S, Almenares SB, Leyva C (2015) Pozzolanic reactivity of low grade kaolinitic clays: influence of mineralogical composition. RILEM Bookseries. <https://doi.org/10.1007/978-94-017-9939-3>
- Taylor-Lange SC, Lamon EL, Riding KA, Juenger MCG (2015) Calcined kaolinite-bentonite clay blends as supplementary cementitious materials. *Appl Clay Sci* 5(108):84–93. <https://doi.org/10.1016/j.clay.2015.01.025>
- Hollanders S, Adriaens R, Skibsted J, Cizer O, Elsen J (2016) Pozzolanic reactivity of pure calcined clays. *Appl Clay Sci* 11(132–133):552–560. <https://doi.org/10.1016/J.CLAY.2016.08.003>
- Avet F, Scrivener K (2018) Investigation of the calcined kaolinite content on the hydration of Limestone Calcined Clay Cement (LC3). *Cem Concr Res* 5(107):124–135. <https://doi.org/10.1016/J.CEMCONRES.2018.02.016>
- Scrivener K, Martirena F, Bishnoi S, Maity S (2018) Calcined clay limestone cements (LC3). *Cem Concr Res* 12(114):49–56. <https://doi.org/10.1016/J.CEMCONRES.2017.08.017>
- Ferreiro S, Herfort D, Damtoft JS (2017) Effect of raw clay type, fineness, water-to-cement ratio and fly ash addition on workability and strength performance of calcined clay - Limestone Portland cements. *Cem Concr Res* 11(101):1–12. <https://doi.org/10.1016/J.CEMCONRES.2017.08.003>
- Dhandapani Y, Sakthivel T, Santhanam M, Gettu R, Pillai RG (2018) Mechanical properties and durability performance of concretes with Limestone Calcined Clay Cement (LC3). <https://doi.org/10.1016/j.cemconres.2018.02.005>
- Scrivener K, Avet F, Maraghechi H, Zunino F, Ston J, Hanpongpun W et al (2018) Impacting factors and properties of limestone calcined clay cements (LC3). *Green Mater* 7(1):3–14. <https://doi.org/10.1680/jgrma.18.00029>
- Sandberg P, Bishnoi S (2018) Sulphate optimization of binders with calcined clay using isothermal calorimetry. RILEM Bookseries. 16:422–426. https://doi.org/10.1007/978-94-024-1207-9_68

11. Barton CD, Karathanasis AD (2002) Clay Minerals. Rattan Lal Comp, ed Encyclopedia of Soil Sciences, New York: Marcel Dekker, 187–192
12. Amin NU, Alam S, Gul S, Muhammad K (2012) Activation of clay in cement mortar applying mechanical, chemical and thermal techniques. *Adv Cem Res* 24(6):319–324. <https://doi.org/10.1680/adcr.11.00020>
13. Alujas A, Fernández R, Quintana R, Scrivener KL, Martirena F (2015) Pozzolanic reactivity of low grade kaolinitic clays: Influence of calcination temperature and impact of calcination products on OPC hydration. *Appl Clay Sci* 5(108):94–101. <https://doi.org/10.1016/J.CLAY.2015.01.028>
14. He C, Osbaeck B, Makovicky E (1995) Pozzolanic reactions of six principal clay minerals: activation, reactivity assessments and technological effects. *Cem Concrete Res* 25(8):1691–1702
15. Poli AL, Batista T, Schmitt CC, Gessner F, Neumann MG (2008) Effect of sonication on the particle size of montmorillonite clays. *J Colloid Interface Sci* 325(2):386–390. <https://doi.org/10.1016/J.JCIS.2008.0.016>
16. Tole I (2022) Enhancing the pozzolanic activity of three natural clays from sweden by mechanochemical activation process. *SSRN Electron J*, 0–2. <https://doi.org/10.2139/ssrn.4100172>
17. Almenares RS, Vizcaíno LM, Damas S, Mathieu A, Alujas A, Martirena F (2017) Industrial calcination of kaolinitic clays to make reactive pozzolans. *Case Stud Constr Mater* 6(6):225–232. <https://doi.org/10.1016/J.CSCM.2017.03.005>
18. Ding S, Zhang L, Ren X, Xu B, Zhang H, Ma F (2012) The characteristics of mechanical grinding on kaolinite structure and thermal behavior. *Energy Procedia*. 16(PART B):1237–1240. <https://doi.org/10.1016/j.egypro.2012.01.197>
19. Fernandez R, Martirena F, Scrivener KL (2011) The origin of the pozzolanic activity of calcined clay minerals. A comparison between kaolinite, illite and montmorillonite. *Cem Concrete Res* 41(1):113–122. <https://doi.org/10.1016/J.CEMCONRES.2010.09.013>
20. Kumar R, Kumar S, Mehrotra SP (2007) Towards sustainable solutions for fly ash through mechanical activation. 52:157–179. <https://doi.org/10.1016/j.resconrec.2007.06.007>
21. Sa PJ, Jime C, Haro D, Pe LA, Varona I, Pe L (2000) Effects of Dry Grinding on the Structural Changes of Kaolinite Powders, 57:1649–1657
22. Baki VA, Ke X, Heath A, Calabria-Holley J, Terzi C, Sirin M (2022) The impact of mechanochemical activation on the physicochemical properties and pozzolanic reactivity of kaolinite, muscovite and montmorillonite. *Cem Concr Res* 162(September):106962. <https://doi.org/10.1016/j.cemconres.2022.106962>
23. Tole I (2022) Ph.D. thesis: revalorization of poorly reactive sources by mechanochemical activation. Luleå University of Technology
24. Ilić B, Radonjanin V, Malešev M, Zdujić M, Mitrović A (2016) Effects of mechanical and thermal activation on pozzolanic activity of kaolin containing mica. *Appl Clay Sci* 123:173–181. <https://doi.org/10.1016/j.clay.2016.01.029>
25. Hanein T, Thienel KC, Zunino F, Marsh ATM, Maier M, Wang B, et al. (2022) Clay calcination technology: state-of-the-art review by the RILEM TC 282-CCL. *Mater Struct/Materiaux et Constr* 55(1). <https://doi.org/10.1617/s11527-021-01807-6>
26. Souiri A, Kazemi-kamyab H, Snellings R, Naghizadeh R, Golestani-fard F, Scrivener K (2015) Cement and Concrete Research Pozzolanic activity of mechanochemically and thermally activated kaolins in cement. *Cem Concr Res* 77:47–59. <https://doi.org/10.1016/j.cemconres.2015.04.017>
27. Vizcayno C, Gutiérrez RMD, Castello R, Rodriguez E, Guerrero CE (2010) Applied clay science pozzolan obtained by mechanochemical and thermal treatments of kaolin. *Appl Clay Sci* 49(4):405–413. <https://doi.org/10.1016/j.clay.2009.09.008>
28. Saikia NJ, Bharali DJ, Sengupta P, Bordoloi D, Goswamee RL, Saikia PC et al (2003) Characterization, beneficiation and utilization of a kaolinite clay from Assam. *India*. 24:93–103. [https://doi.org/10.1016/S0169-1317\(03\)00151-0](https://doi.org/10.1016/S0169-1317(03)00151-0)
29. Vizcayno C, de Gutiérrez RM, Castello R, Rodriguez E, Guerrero CE (2010) Pozzolan obtained by mechanochemical and thermal treatments of kaolin. *Appl Clay Sci* 49(4):405–413. <https://doi.org/10.1016/j.clay.2009.09.008>
30. Zunino F, Boehm-Courjault E, Scrivener K (2020) The impact of calcite impurities in clays containing kaolinite on their reactivity in cement after calcination. *Mater Struct/Mater et Constr*; 53(2). <https://doi.org/10.1617/s11527-020-01478-9>
31. Sanchez-Soto PJ, Haro M, Perez-Maqueda LA, Varona I, Perez-Rodriguez J (2000) Effects of dry grinding on the structural changes of kaolinite powders, 57:1649–1657
32. Danner T (2013) Reactivity of calcined clays. NTNU
33. Alujas Diaz A, Almenares Reyes RS, Hanein T, Irassar EF, Juenger M, Kanavaris F, et al (2022) Properties and occurrence of clay resources for use as supplementary cementitious materials: a paper of RILEM TC 282-CCL. *Mater Struct/Materiaux et Constr* 55(5). <https://doi.org/10.1617/s11527-022-01972-2>
34. Maier M, Beuntner N (2020) Thienel KC (2021) Applied clay science mineralogical characterization and reactivity test of common clays suitable as supplementary cementitious material. *Appl Clay Sci* 2021(202):105990. <https://doi.org/10.1016/j.clay.2021.105990>
35. Londono-Zuluaga D, Gholizadeh-Vayghan A, Winnefeld F, Avet F, Ben Haha M, Bernal SA, et al (2022) Report of RILEM TC 267-TRM phase 3: validation of the R3 reactivity test across a wide range of materials. *Mater Struct* 55(5). <https://doi.org/10.1617/s11527-022-01947-3>
36. Plusquellec G, Babaahmadi A, L'Hopital E, Mueller U (2021) Activated clays as supplementary cementitious material
37. Danner T, Norden G, Justnes H (2018) Characterisation of calcined raw clays suitable as supplementary cementitious materials. *Appl Clay Sci* 162(April):391–402. <https://doi.org/10.1016/j.clay.2018.06.030>
38. Snellings R, Almenares R, Theodore R, Irassar EF, Kanavaris F, Maier M, et al. (2022) Paper of RILEM TC 282-CCL: mineralogical characterization methods for clay



- resources intended for use as supplementary cementitious material. vol. 1. Springer Netherlands. Available from: <https://DOIurl.org/10.1617/s11527-022-01973-1>
39. Suraneni P, Weiss J (2017) Examining the pozzolanicity of supplementary cementitious materials using isothermal calorimetry and thermogravimetric analysis. *Cement Concr Compos* 10(83):273–278. <https://doi.org/10.1016/J.CEMCONCOMP.2017.07.009>
 40. Mark U, Anyakwo CN, Onyemaobi OO, Nwobodo CS (2019) Determination of the calcination procedure required to activate edda clay for optimal leaching of alumina. *J Miner Mate Char Eng* 07(02):49–63. <https://doi.org/10.4236/jmmce.2019.72004>
 41. Tole I, Habermehl-cwirzen K, Rajczakowska M, Cwirzen A (2018) Activation of a raw clay by mechanochemical process—effects of various parameters on the process efficiency and cementitious properties, 6–8. <https://doi.org/10.3390/ma11101860>
 42. Maleki S, Karimi-Jashni A (2017) Effect of ball milling process on the structure of local clay and its adsorption performance for Ni(II) removal. *Appl Clay Sci* 137:213–224. <https://doi.org/10.1016/j.clay.2016.12.008>
 43. Zanelli C, Iglesias C, Domínguez E, Gardini D, Raimondo M, Guarini G et al (2015) Mineralogical composition and particle size distribution as a key to understand the technological properties of Ukrainian ball clays. *Appl Clay Sci* 5(108):102–110. <https://doi.org/10.1016/j.clay.2015.02.005>
 44. Fitos M, Badogiannis EG, Tsvilis SG, Perraki M (2015) Pozzolanic activity of thermally and mechanically treated kaolins of hydrothermal origin. *Appl Clay Sci* 116–117:182–192. <https://doi.org/10.1016/j.clay.2015.08.028>
 45. Karunadasa KSP, Manoratne CH, Pitawala HMTGA, Rajapakse RMG (2019) Thermal decomposition of calcium carbonate (calcite polymorph) as examined by in-situ high-temperature X-ray powder diffraction. *J Phys Chem Solids* 134(May):21–28. <https://doi.org/10.1016/j.jpcs.2019.05.023>
 46. Kuila U, Prasad M (2013) Specific surface area and pore-size distribution in clays and shales. 341–362. <https://doi.org/10.1111/1365-2478.12028>
 47. Yanguatin H, Ramírez JH, Tironi A, Tobón JI (2019) Effect of thermal treatment on pozzolanic activity of excavated waste clays. *Constr Build Mater* 211:814–823. <https://doi.org/10.1016/j.conbuildmat.2019.03.300>
 48. Shui K, Yuan K, Sun T, Li Q, Zeng W (2015) Calcined clays for sustainable concrete
 49. Johnston CJ, Pepper RA, Martens WN Couperthwaite S (2022) Improvement of aluminium extraction from low-grade kaolinite by iron oxide impurities: Role of clay chemistry and morphology. *Miner Eng* 176(Dec 2021):107346. <https://doi.org/10.1016/j.mineng.2021.107346>
 50. Erlström M, Pusch R (1987) Survey of Swedish buffer material candidates and methods for characterization
 51. Ortega A, Gotor FJ (2010) The multistep nature of the kaolinite dehydroxylation: kinetics and mechanism 203(26073):197–203. <https://doi.org/10.1111/j.1551-2916.2009.03328.x>
 52. Garg N, Skibsted J (2015) Pozzolanic reactivity of a calcined interstratified illite/smectite. *Cem Concr Res*. <https://doi.org/10.1016/j.cemconres.2015.08.006>
 53. Snellings R, Li X, Avet F, Scrivener K (2019) Rapid, robust, and relevant (R3) reactivity test for supplementary cementitious materials. *ACI Mater J* 116(4):155–162. <https://doi.org/10.14359/51716719>

Publisher's Note Springer Nature remains neutral with regard to jurisdictional claims in published maps and institutional affiliations.

